Inorg. Chem. **2003**, *42*, 3642–3649

New One-Dimensional Azido-Bridged Manganese(II) Coordination Polymers Exhibiting Alternating Ferromagnetic–Antiferromagnetic Interactions: Structural and Magnetic Studies

En-Qing Gao,[†,‡] Shi-Qiang Bai,[†,‡] Yan-Feng Yue,[‡] Zhe-Ming Wang,[†] and Chun-Hua Yan*[,†]

State Key Lab of Rare Earth Materials Chemistry and Applications and PKU-HKU Joint Lab on Rare Earth Materials and Bioinorganic Chemistry, Peking University, Beijing 100871, China, and Department of Chemistry, Qufu Normal University, Qufu 273165, Shandong, China

Received December 23, 2002

Five Mn(II)–azido coordination polymers of formula $[Mn(L)(N_3)_2]_n$ have been synthesized and crystallographically characterized, and their magnetic properties studied, where L's are the bidentate Schiff bases obtained from the condensation of pyridine-2-carbaldehyde with aniline (**1**) and its derivatives *p*-toluidine (**2**), *m*-toluidine (**3**), *p*-chloroaniline (**4**), and *m*-chloroaniline (**5**). All the complexes consist of the zigzag Mn(II)–azido chains in which the Mn(II) ions are alternately bridged by two end-to-end (EE) and two end-on (EO) azido ligands, the *cis*-octahedral coordination being completed by the two nitrogen atoms of the Schiff base ligands. Compound **2** is unique in that the Mn–(EE-N_3)$_2$–Mn ring adopts an unusual twist conformation with the two linear azido bridges crossing each other. By contrast, the rings in the other compounds take the usual chair conformation with the two azido bridges parallel. The double EO bridging fragments in the complexes are similar with the bridging angles (Mn–N–Mn) ranging from 99.6° to 104.0°. Magnetic analyses reveal that alternating ferro- and antiferromagnetic interactions are mediated through the alternating EO and EE azido bridges with the J_F and J_{AF} parameters in the ranges of 4.1–8.0 and –11.8 to –15.4 cm^{-1}, respectively. Finally, the magnetostructural correlations are investigated. The present complexes follow the general trend that the ferromagnetic interaction through the double EO bridge increases with the Mn–N–Mn bridging angle, while the antiferromagnetic interaction through the double EE bridge is dependent on the distortion of the Mn–$(N_3)_2$–Mn ring from planarity toward the chair conformation and the Mn–N–N angle.

Introduction

The design and magnetism of discrete polynuclear molecules and molecule-based coordination polymers with one- or multiple-dimensional structures are currently of considerable interest, not only for understanding the fundamental science of magnetic interactions and magnetostructural correlations in molecular systems, but also for developing new functional molecule-based materials.[1,2] In this context, azido-bridged complexes have received intense attention due to their structural and magnetic diversities.[3]

As a versatile bridging ligand and an efficient mediator for magnetic coupling, the azido ion has been shown to be able to link two or more metal ions in various modes, μ-1,1 (end-on, EO),[3] μ-1,3 (end-to-end, EE),[3] μ-1,1,3,[4] and others,[5] giving rise to a variety of zero-, one-, two-, and three-dimensional polynuclear complexes.[3−9] The remarkable structural variations of azido complexes have resulted in a diversity of magnetic behaviors. It has been established that

* Author to whom correspondence should be addressed. E-mail: chyan@chem.pku.edu.cn. Fax: +86-10-62754179.
† Peking University.
‡ Qufu Normal University.

(1) Kahn, O. *Molecular Magnetism*; VCH: New York, 1993.
(2) Miller, J. S. *Inorg. Chem.* **2000**, *39*, 4392
(3) Ribas, J.; Escuer, A.; Monfort, M.; Vicente, R.; Cortés, R.; Lezama, L.; Rojo, T. *Coord. Chem. Rev.* **1999**, *193*−*195*, 1027 and references therein.
(4) (a) Ribas, J.; Monfort, M.; Solans, X.; Drillon, M. *Inorg. Chem.* **1994**, *33*, 742. (b) Serna, Z. E.; Lezama, L.; Urtiaga, M. K.; Arriortua, M. I.; Barandika, M. G. B.; Cortés, R.; Rojo, T. *Angew. Chem., Int. Ed.* **2000**, *39*, 344. (c) Zhang, L.; Tang, L.-F.; Wang, Z.-H.; Du, M.; Julve, M.; Lloret, F.; Wang, J.-T. *Inorg. Chem.* **2001**, *40*, 3619.
(5) (a) Guo, G.-C.; Mak, T. C. W. *Angew. Chem., Int. Ed.* **1998**, *37*, 3286. (b) Halcrow, M. A.; Sun, J.-S.; Huffman, J. C.; Christou G. *Inorg. Chem.* **1995**, *34*, 4167. (c) Papaefstathiou, G. S.; Perlepes, S. P.; Escuer, A.; Vicente, R.; Font-Bardia, M.; Solans, X. *Angew. Chem., Int. Ed.* **2001**, *40*, 884. (d) Goher, M. A. S.; Cano, J.; Journaux, Y.; Abu-Youssef, M. A. M.; Mautner, F. A.; Escuer, A.; Vicente, R. *Chem.—Eur. J.* **2000**, *6*, 778.

10.1021/ic0262987 CCC: $25.00
Published on Web 05/09/2003

the magnetic coupling mediated by the azido bridge is generally ferromagnetic (F) for the EO mode and antiferromagnetic (AF) for the EE mode, but an increasing number of exceptions have been reported recently.[10,11] For the bulk magnetic properties, different phenomena, including ferromagnetism,[11,12] antiferromagnetism,[9b] metamagnetism,[8a,b,13] weak ferromagnetism,[8a,14] and paramagnetism, have been recognized in azido-bridged coordination polymers. Furthermore, the structural and magnetic diversities of azido-bridged complexes are enhanced by the observation that different coordination modes can simultaneously exist within the same species. In one-dimensional (1D) systems, for instance, different combinations of EO and EE modes have resulted in some unusual alternating chains along which the magnetic coupling changes its sign according to a certain sequence such as AF−F,[3,15−17] AF−AF−F[18] (ferrimagnetic), AF−F−F−F,[19] or even AF−F−F−F−F. [18a]

As far as 1D structures are concerned, the number of Mn(II)−azido systems[16−18] that are structurally and magnetically characterized is rather limited compared to those of Cu(II) and Ni(II) analogues. To our knowledge, only five Mn(II)−azido chains with alternating double EE and double EO bridges have been reported in the literature.[17] Studies on magnetostructural correlations for these complexes have shown both agreement and disagreement between theoretical and experimental results, and therefore, more examples are highly desired to get a deeper understanding of the correlations. With this in mind, we here report the synthesis, structural characterization, and magnetic properties of five 1D Mn(II) complexes of general formula $[Mn(L^i)(N_3)_2]_n$ ($i = 1-5$), where L^1 to L^5 are the bidentate Schiff bases obtained from the condensation of 2-pyridylaldehyde with aniline, *p*-toluidine, *m*-toluidine, *p*-chloroaniline, and *m*-chloroaniline, respectively. These compounds represent new examples of 1D Mn(II)−azido complexes with alternating double EE and double EO bridges. They are similar in local coordination environments but somewhat different in bridging parameters and, therefore, should be appropriate for magnetostructural studies.

Experimental Section

Materials and Synthesis. All the starting chemicals were of AR grade and used as received. The Schiff bases were prepared in situ according to the literature methods for analogous compounds.[20]

Caution! Although not encountered in our experiments, azido complexes of metal ions are potentially explosive. Only a small amount of the material should be prepared, and it should be handled with care.

$[Mn(L^1)(N_3)_2]_n$ (1). A mixture of pyridine-2-carbaldehyde (0.055 g, 0.5 mmol) and aniline (0.046 g, 0.5 mmol) in 10 mL of methanol was refluxed for 2 h to obtain a yellow solution of the Schiff base, and then a methanolic solution (10 mL) containing manganese(II) perchlorate hexahydrate (0.181 g, 0.5 mmol) and sodium azide (0.065 g, 1 mmol) was added with continuous stirring. Slow evaporation of the resulting orange solution at room temperature yielded orange crystals of **1** within 1 week. Yield: 34.8%. Anal. Calcd for $C_{12}H_{10}N_8Mn$: C, 44.87; H, 3.14; N, 34.89. Found: C, 44.72; H, 3.32; N, 34.64. Main IR bands: 2098vs, 2060vs, 1591m, 1489m, 1442m, 1330m, 1014m, 922m, 781m, 744m, 691m.

$[Mn(L^2)(N_3)_2]_n$ (2). The complex was prepared in the same way as **1**, using *p*-toluidine instead of aniline. Yield: 31.7%. Anal. Calcd

(6) (a) Manikandan, P.; Muthukumaran, R.; Justin Thomas, K. R.; Varghese, B.; Chandramouli, G. V. R.; Manoharan, P. T. *Inorg. Chem.* **2001**, *40*, 2378. (b) Escuer, A.; Goher, M. A. S.; Mautner, F. A.; Vicente, R. *Inorg. Chem*. **2000**, *39*, 2107.

(7) (a) Monfort, M.; Resino, I.; El Fallah, M. S.; Ribas, J.; Solans, X.; Font-Bardia, M.; Stoeckli-Evans, H. *Chem.—Eur. J.* **2001**, *7*, 280. (b) Hernández, M. L.; Barandika, M. G.; Urtiaga, M. K.; Cortés, R.; Lezama, L.; Arriortua, M. I. *J. Chem. Soc., Dalton Trans*. **2000**, 79.

(8) (a) Escuer, A.; Cano, J.; Goher, M. A. S.; Journaux, Y.; Lloret, F.; Mautner F. A.; Vicente, R. *Inorg. Chem.* **2000**, *39*, 4688. (b) Monfort, M.; Resino, I.; Ribas, J.; Stoeckli-Evans, H. *Angew. Chem., Int. Ed*. **2000**, *39*, 191. (c) Goher, M. A. S.; Abu-Youssef, M. A.; Mautner, F. A.; Vicente, R.; Escuer, A. *Eur. J. Inorg. Chem.* **2000**, 1819.

(9) (a) Goher, M. A. S.; Mautner, F. A. *Croat. Chim. Acta* **1990**, *63*, 559. (b) Mautner, F. A.; Hanna, S.; Cortés, R.; Lezama, L.; Barandika, M. G.; Rojo, T. *Inorg. Chem*. **1999**, *38*, 4647.

(10) (a) Tandon, S. S.; Thompson, L. K.; Manuel, M. E.; Bridson, J. N. *Inorg. Chem.* **1994**, *33*, 5555. (b) Mukherjee, P. S.; Maji, T. K.; Mostafa, G.; Mallah, T., Chaudhuri, N. R. *Inorg. Chem*. **2000**, *39*, 5147. (c) Xie, Y.; Liu, Q.; Jiang, H.; Du, C.; Xu, X.; Yu, M.; Zhu, Y. *New J. Chem*. **2002**, *26*, 176. (d) Escuer, A.; Harding, C. J.; Dussart, Y.; Nelson, J.; McKee, V.; Vicente, R. *J. Chem. Soc., Dalton Trans*. **1999**, 223. (e) Maji, T. K.; Mukherjee, P. S.; Mostafa, G.; Mallah, T.; Cano-Boquera, J.; Chaudhuri, N. R *Chem. Commun*. **2001**, 1012. (f) Mukherjee, P. S.; Dalai, S.; Mostafa, G.; Lu, T. H.; Rentschler, E.; Chaudhuri, N. R *New J. Chem*. **2001**, *25*, 1203. (g) Dalai, S.; Mukherjee, P. S.; Mallah, T.; Drew, M. G. B.; Chaudhuri, N. R. *Inorg. Chem. Commun*. **2002**, *5*, 472. (h) Mukherjee, P. S.; Maji, T. P.; Escuer, A.; Vicente, R.; Ribas, J.; Rosair, G.; Mautner, F. A.; Chaudhuri, N. R. *Eur. J. Inorg. Chem*. **2002**, 943. (i) Hong, C. S.; Do, Y. *Angew. Chem., Int. Ed*. **1999**, *38*, 193. (j) Mukherjee, P. S.; Dalai, S.; Zangrando, E.; Lloret, F.; Chaudhuri, N. R *Chem. Commun*. **2001**, 1444.

(11) (b) Shen, Z.; Zuo, J.-L.; Gao, S.; Song, Y.; Che, C.-M.; Fun, H.-K.; You, X.-Z. *Angew. Chem., Int. Ed*. **2000**, *39*, 3633. (c) Hong, C. S.; Koo, J.; Son, S.-K.; Lee, Y. S.; Kim, Y.-S.; Do, Y. *Chem.—Eur. J*. **2001**, *7*, 4243.

(12) Fu, A. H.; Huang, X. Y.; Li, J.; Yuen, T.; Lin, C. L. *Chem.—Eur. J*. **2002**, *8*, 2239.

(13) Hao, X.; Wei Y.; Zhang, S. *Chem. Commun.* **2000**, 2271.

(14) (a) Han, S.; Manson, J. L.; Kim, J.; Miller, *J. Inorg. Chem*. **2000**, *39*, 4182. (b) Martin, S.; Barandika, M. G.; Lezama, L.; Pizarro, J. L.; Serna, Z. E.; de Larramendi, J. I. R.; Arriortua, M. I.; Rojo, T.;. Cortés, R. *Inorg. Chem*. **2001**, *40*, 4109. (c) Escuer, A.; Vicente, R.; Goher, M. A. S.; Mautner, F. A. *Inorg. Chem*. **1997**, *36*, 3440.

(15) (a) Viau, G.; Lombardi, M. G.; De Munno, G.; Julve, M.; Lloret, F.; Faus, J.; Caneschi, A.; Clemente-Juan, J. M. *J. Chem. Soc., Chem. Commun*. **1997**, 1195. (b) Shen, H.-Y.; Bu, W.-M.; Gao, E.-Q.; Liao, D.-Z.; Jiang, Z.-H.; Yan, S.-P.; Wang, G.-L. *Inorg. Chem*. **2000**, *39*, 396. (c) Monfort, M.; Resino, I.; Ribas, J.; Solans, X.; Font-Bardia, M.; Rabu, P.; Drillon, M. *Inorg. Chem*. **2000**, *39*, 2572. (d) Shen, Z.; Zuo, J. L.; Yu, Z.; Zhang, Y.; Bai, J. F.; Che, C. M.; Fun, H. K.; Vittal, J. J.; You, X. Z. *J. Chem. Soc., Dalton Trans*. **1999**, 3393.

(16) (a) Escuer, A.; Vicente, R.; Goher, M. A. S.; Mautner, F. A. *Inorg. Chem*. **1998**, *37*, 782. (b) Sra, A. K.; Sutter, J.-P.; Guionneau, P.; Chasseau, D.; Yakhmi, J. V.; Kahn, O. *Inorg. Chim. Acta* **2000**, *300−302*, 778. (c) Abu-Youssef, M.; Escuer, A.; Goher, M. A. S.; Mautner, F. A.; Vicente, R. *J. Chem. Soc., Dalton Trans*. **2000**, 413. (d) Cortés, R.; Lezama, L.; Pizarro, J. L.; Arriortua, M. I.; Solans, X.; Rojo, T. *Angew. Chem., Int. Ed. Engl*. **1994**, *33*, 2488.

(17) (a) Abu-Youssef, M. A.; Escuer, A.; Gatteschi, D.; Goher, M. A. S.; Mautner, F. A.; Vicente, R. *Inorg. Chem*. **1999**, *38*, 5716. (b) Cortés, R.; Drillon, M.; Solans, X.; Lezama, L.; Rojo, T. *Inorg. Chem*. **1997**, *36*, 677. (c) Abu-Youssef, M.; Escuer, A.; Goher, M. A. S.; Mautner, F. A.; Vicente, R. *Eur. J. Inorg. Chem*. **1999**, 687. (d) Tang, L.-F.; Zhang, L.; Li, L.-C.; Cheng, P.; Wang, Z.-H.; Wang, J.-T. *Inorg. Chem*. **1999**, *38*, 6326. (e) Villanueva, M.; Mesa, J. L.; Urtiaga, M. K.; Cortés, R.; Lezama, L.; Arriortua, M. I.; Rojo, T. *Eur. J. Inorg. Chem*. **2001**, 1581.

(18) (a) Abu-Youssef, M.; Escuer, A.; Goher, M. A. S.; Mautner, F. A.; Reiss, G.; Vicente, R. *Angew. Chem., Int. Ed.* **2000**, *39*, 1624. (b) Abu-Youssef, M. A. M.; Drillon, M.; Escuer, A.; Goher, M. A. S.; Mautner, F. A.; Vicente, R. *Inorg. Chem.* **2000**, *39*, 5022.

(19) Ribas, J.; Monfort, M.; Resino, I.; Solans, X.; Rabu, P.; Maingot, F.; Drillon, M. *Angew. Chem., Int. Ed. Engl.* **1996**, *35*, 2520.

(20) Bamfield, P.; Price, R.; Miller, R. G. J. *J. Chem. Soc. A* **1969**, 1447.

Table 1. Summary of Crystallographic Data for the Complexes

	1	2	3	4	5
emprical formula	$C_{12}H_{10}MnN_8$	$C_{13}H_{12}MnN_8$	$C_{13}H_{12}MnN_8$	$C_{12}H_9ClMnN_8$	$C_{12}H_9ClMnN_8$
fw	321.22	335.25	335.25	355.66	355.66
cryst syst	monoclinic	triclinic	triclinic	triclinic	triclinic
space group	$P2_1/c$	$P\bar{1}$	$P\bar{1}$	$P\bar{1}$	$P\bar{1}$
a, Å	7.6732(2)	10.5952(3)	7.4692(2)	8.0054(2)	7.5390(3)
b, Å	10.1040(3)	12.3357(3)	9.9908(4)	9.7308(3)	9.7950(4)
c, Å	17.9135(7)	12.9904(4)	10.3615(5)	9.9532(3)	10.5164(5)
α, deg		103.4941(15)	97.598(2)	74.5845(15)	99.8150(16)
β, deg	98.4536(11)	113.9738(16)	99.091(2)	76.4177(13)	97.3533(17)
γ, deg		97.7399(14)	101.330(2)	83.2995(15)	100.496(3)
V, Å^3	1373.74(8)	1457.35(7)	737.90(5)	725.33(4)	742.20(6)
Z	4	4	2	2	2
D_c, g/cm3	1.553	1.528	1.509	1.628	1.591
μ(Mo Kα), mm^{-1}	0.967	0.915	0.904	1.103	1.077
T, K	293(2)	293(2)	293(2)	293(2)	293(2)
θ range, deg	3.42−27.50	3.40−27.44	3.63−27.51	3.43−27.46	3.68−27.12
no. of reflns measd	24067	26350	13540	14372	13538
no. of unique reflns/R_{int}	3128/0.0634	6410/0.0950	3312/0.0611	3222/0.0559	3258/0.0501
no. of params refined	190	397	199	199	200
R1[a] [$I > 2\sigma(I)$]	0.0442	0.0468	0.0414	0.0377	0.0453
wR2[b] (all data)	0.1020	0.1038	0.0991	0.0921	0.1207
GOF on F^2	1.090	0.999	1.004	1.022	1.015
ρ_{max}/ρ_{min}, e Å^{-3}	0.349/−0.427	0.336/−0.355	0.282/−0.333	0.279/−0.383	0.671/−0.283

[a] $R1 = \sum||F_o| - |F_c||/\sum|F_o|$. [b] $wR2 = \{\sum[w(F_o^2 - F_c^2)^2]/\sum[w(F_o^2)^2]\}^{1/2}$.

for $C_{13}H_{13}N_8Mn$: C, 46.44; H, 3.90; N, 33.33. Found: C, 46.30; H, 3.65; N, 33.09. Main IR bands: 2095vs, 2065vs, 1588m, 1508m, 1442m, 1338m, 1015m, 823m, 769m.

$[Mn(L^3)(N_3)_2]_n$ (3). The complex was prepared in the same way as **1**, using *m*-toluidine instead of aniline. Yield: 36.9%. Anal. Calcd for $C_{13}H_{13}N_8Mn$: C, 46.44; H, 3.90; N, 33.33. Found: C, 46.42; H, 3.71; N, 33.10. Main IR bands: 2103vs, 2056vs, 1592m, 1440m, 1338m, 1013m, 788m, 771m, 688m.

$[Mn(L_4)(N_3)_2]_n$ (4). The complex was prepared in the same way as **1**, using *p*-chloroanline instead of aniline. Yield: 35.8%. Anal. Calcd for $C_{12}H_9ClN_8Mn$: C, 40.55; H, 2.55; N, 31.51. Found: C, 40.39; H, 2.53; N, 31.41. Main IR bands: 2099vs, 2066vs, 1593m, 1485m, 1440m, 1336m, 1094m, 1013m, 833m, 775m.

$[Mn(L_5)(N_3)_2]_n$ (5). The complex was prepared in the same way as **1**, using *m*-chloroanline instead of aniline. Yield: 33.8%. Anal. Calcd for $C_{12}H_9ClN_8Mn$: C, 40.55; H, 2.55; N, 31.51. Found: C, 40.28; H, 2.59; N, 31.29. Main IR bands: 2105vs, 2062vs, 1592m, 1585m, 1480m, 1442m, 1339m, 1013m, 922m, 874m, 786m, 678m.

Physical Measurements. Elemental analyses (C, H, N) were performed on a Perkin-Elmer 240 analyzer. IR spectra were recorded on a Nicolet Magna-IR 750 spectrometer equipped with a Nic-Plan microscope. Variable-temperature magnetic susceptibilities were measured on an Oxford MagLab 2000 magnetometer. Diamagnetic corrections were made with Pascal's constants for all the constituent atoms.[21]

Crystallographic Studies. Diffraction intensity data for single crystals of **1**−**5** were collected at room temperature on a Nonius Kappa CCD area detector equipped with graphite-monochromated Mo Kα radiation ($\lambda = 0.71073$ Å). Empirical absorption corrections were applied using the Sortav program.[22] The structure was solved by the direct method and refined by the full-matrix least-squares method on F^2 with anisotropic thermal parameters for all non-hydrogen atoms.[23] Hydrogen atoms were located geometrically and refined isotropically. Pertinent crystallographic data and structure refinement parameters are summarized in Table 1.

Results and Discussion

Syntheses and IR Spectra. The five complexes were synthesized as crystals by reacting $Mn(ClO_4)_2$ and NaN_3 with the appropriate Schiff bases prepared in situ in methanol. The IR spectra of these complexes are quite similar. In the 2000−2100 cm^{-1} region expected for the $\nu_{as}(N_3)$ absorption, the occurrence of two sharp and strong bands at about 2060 and 2100 cm^{-1} indicates the presence of two different azido groups. The band of higher frequency is attributed to the EO bridge and the other to the EE bridge.[10a,17b] The medium band at ca. 1335 cm^{-1} is assignable to the azido symmetric stretching mode, $\nu_s(N_3)$, for the EO bridges. The ν(C═N) absorption characteristic of the Schiff base ligands occurs at ca. 1590 cm^{-1} as a medium band.

Despite the large number of M(II)−azido complexes reported to date, no correlation has been found between the properties of the coligand and the coordination mode of the azido ligand or the polymeric topology of the resulting complex.[3] Indeed, the reported Mn(II)−azido complexes of general formula $[Mn(L)_2(N_3)_2]_n$, where L's are monodentate pyridine and its derivatives, exhibit a variety of structures with different bridging modes or different polymeric dimensionalities,[3,8a,9,14c,17,18] and synthetically it is impossible to determine, with our present state of knowledge, which bridging mode or polymeric topology will be adopted with a specific ligand. However, when bidentate chelating coligands are used, nearly all the reported Mn(II)−azido polymers, of formula $[Mn(L)(N_3)_2]_n$ (L = 2,2′-bipyridine,[17a] bis(pyrazol-1-yl)methane,[17d] and 2,2′-dipyridylamine[17e]), exhibit 1D zigzag chain structures with alternating double EO and double EE bridges. The only exception is $[Mn(dmbpy)(N_3)_2]_n$ (dmbpy = 4,4′-dimethyl-2,2′-bipyridine), where a 2D network with alternating single EE and double EO bridges

(21) O'Connor, C. J. *Prog. Inorg. Chem.* **1982**, *29*, 203.
(22) (a) Blessing, R. H. *Acta Crystallogr.* **1995**, *A51*, 33. (b) Blessing, R. H. *J. Appl. Crystallogr.* **1997**, *30*, 421.
(23) (a) Sheldrick, G. M. *SHELXTL*, Version 5.1; Bruker Analytical X-ray Instruments Inc.: Madison, WI, 1998. (b) Sheldrick, G. M. *SHELXL-97*, PC Version; University of Göttingen: Göttingen, Germany, 1997.

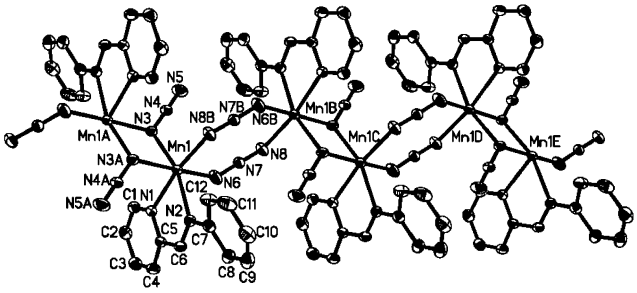

Figure 1. ORTEP view of the chain structure in **1** with the atom labeling scheme.

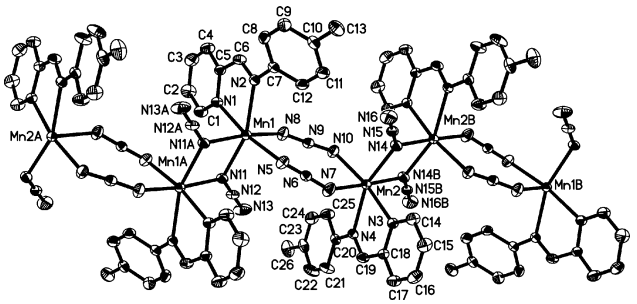

Figure 2. ORTEP view of the chain structure in **2** with the atom labeling scheme.

Table 2. Selected Bond Distances (Å) and Angles (deg) for Complexes **1**, **3**, **4**, and **5**[a]

	1	**3**	**4**	**5**
Mn1−N1	2.273(2)	2.280(2)	2.2575(19)	2.285(3)
Mn1−N2	2.335(2)	2.341(2)	2.3884(18)	2.344(2)
Mn1−N3	2.225(2)	2.233(2)	2.2183(19)	2.231(3)
Mn1−N6	2.224(3)	2.182(2)	2.212(2)	2.184(3)
Mn1−N3A	2.232(2)	2.234(2)	2.2168(19)	2.223(3)
Mn1−N8B	2.172(2)	2.207(2)	2.208(2)	2.194(3)
N3−N4	1.203(3)	1.198(3)	1.194(3)	1.194(3)
N4−N5	1.143(3)	1.144(3)	1.144(3)	1.147(4)
N6−N7	1.168(3)	1.169(3)	1.163(3)	1.167(3)
N7−N8	1.164(3)	1.165(3)	1.159(3)	1.149(4)
N1−Mn1−N2	73.09(8)	72.34(7)	72.69(7)	72.23(9)
N3−Mn1−N1	92.12(8)	164.73(7)	91.40(7)	164.63(10)
N3−Mn1−N2	162.78(8)	111.79(8)	161.79(7)	110.56(9)
N3−Mn1−N6	93.78(10)	93.01(8)	98.60(9)	91.72(11)
N3−Mn1−N3A	80.35(9)	76.12(8)	79.36(8)	76.03(11)
N3−Mn1−N8B	94.62(10)	91.62(9)	93.23(8)	92.22(12)
N6−Mn1−N1	83.12(9)	102.08(8)	85.46(8)	103.63(11)
N6−Mn1−N2	93.14(10)	85.06(8)	89.11(9)	85.11(9)
N6−Mn1−N3A	173.55(10)	166.14(9)	177.32(9)	165.79(11)
N6−Mn1−N8B	90.92(10)	91.79(9)	87.92(8)	91.61(11)
N3A−Mn1−N1	94.36(8)	89.28(7)	96.29(7)	88.84(10)
N3A−Mn1−N2	91.79(8)	90.97(7)	93.34(7)	92.39(9)
N3A−Mn1−N8B	92.21(9)	97.02(8)	90.46(8)	95.99(11)
N8B−Mn1−N1	171.29(9)	85.64(9)	172.43(7)	86.59(11)
N8B−Mn1−N2	101.02(10)	156.49(9)	103.56(8)	157.05(12)
Mn1−N3−Mn1A	99.65(9)	103.88(8)	100.64(8)	103.97(11)
N4−N3−Mn1A	122.32(18)	128.31(17)	128.37(15)	127.2(2)
N4−N3−Mn1	122.07(19)	124.07(16)	130.13(15)	125.9(2)
N7−N8−Mn1B	133.4(2)	133.20(19)	133.11(17)	137.5(3)
N7−N6−Mn1	130.7(2)	126.51(18)	134.73(18)	125.7(2)
N5−N4−N3	178.5(3)	179.1(3)	179.7(4)	179.3(3)
N8−N7−N6	176.6(3)	177.4(3)	177.4(2)	177.2(3)

[a] Symmetry codes: A, $-x+1, -y+2, -z$; B, $-x, -y+2, -z$ for **1**; A, $-x, -y+1, -z+1$; B, $-x+1, -y+1, -z+1$ for **3**−**5**.

is formed.[16d] As revealed by X-ray crystallographic analyses (vide infra), the present five complexes with bidentate Schiff bases as coligands exhibit the general 1D alternating structures.

Description of the Structures. The structure of **1** consists of parallel zigzag chains running parallel to the *a* direction. A perspective view of the chain structure is depicted in Figure 1, and selected bond lengths and angles are listed in Table 2. The adjacent Mn(II) ions in a chain are related by inversion centers and linked alternately by double end-on and double end-to-end azido bridges with the Mn−N distances in the 2.172(2)−2.232(2) Å range. The EO azido bridges show asymmetric N−N distances [1.203(3) vs 1.143(3) Å], while the EE bridges are essentially symmetric [1.168(3) vs 1.164(3) Å]. The *cis*-octahedral coordination polyhedron around Mn(II) is completed by the two nitrogen atoms (N1 and N2) from the chelating Schiff base with longer Mn−N distances [2.272(2) and 2.335(2) Å]. The rather small bite angle [N1−Mn1−N2 = 73.09(8)°] of the Schiff base ligand defines the largest distortion of the geometry. In the double EO bridged $Mn(N_3)_2Mn$ moiety, the Mn1−N3−Mn1A−N3A ring is strictly planar due to the existence of the inversion center. The Mn···Mn distance is 3.406(3) Å, and the Mn1−N3−Mn1A angle is 99.65(9)°, which is among the lowest values for Mn(II) ions with EO azido bridges (100−105°). In the EE bridging moiety, the Mn−N−N angles are 130.7(2)° for Mn1−N6−N7 and 133.4(2)° for Mn1B−N8−N7. The Mn−azido−Mn torsion angle τ, defined by the dihedral angle between the mean planes of Mn1−N6−N7−N8 and Mn1B−N8−N7−N6, is 19.2(3)°. The two EE azido bridges are parallel and thus form a plane, which is characteristic of nearly all polynuclear complexes with double EE azido bridges. The Mn(II) ions are 0.263(5) Å out of the (EE-N_3)$_2$ plane, and the dihedral angle δ between this plane and the N6−Mn1−N8B plane is only 9.8(2)°, indicating only a slight chair conformation for the Mn−$(N_3)_2$−Mn ring. Both τ and δ in **1** are significantly lower than the corresponding angles (40−64° for τ and 20−35° for δ) for previous Mn(II) chains with alternating EE and EO bridges,[18] but comparable to those observed in [Mn(3-Etpy)$_2$(N$_3$)$_2$]$_n$ (3-Etpy = 3-ethylpyridine),[16a] an alternating chain compound with only double EE azido bridges. The Mn···Mn distance for the EE bridge is 5.394(3) Å. The shortest interchain Mn···Mn distance is 8.520 Å between Mn1 and Mn1($1-x, 1-y, z$).

The introduction of a methyl group in the *para* position of the phenyl ring into the Schiff base ligand led to the formation of compound **2**, which crystallized in a different crystal system (Table 1). A perspective view of the structure is depicted in Figure 2, and selected bond lengths and angles are listed in Table 3. The structure of **2** also consists of parallel zigzag chains running along the [011] crystallographic direction, with alternating EE and EO azido bridges. The overall structure of the chain and the local coordination environment around the Mn(II) ion are similar to those of **1**, but now there are no inversion centers in the double EE moieties and the asymmetric unit is doubled (Figure 2). Without the inversion center, the two EE azido bridges are not parallel but cross each other at an angle of 12.0°, yielding an unusual twist conformation for the Mn−$(N_3)_2$−Mn ring. The different conformations of the double EE bridging skeletons in **1** and **2** are compared in Figure 3.

Table 3. Selected Bond Distances (Å) and Angles (deg) for **2**[a]

Mn1−N5	2.199(3)	Mn2−N10	2.199(3)
Mn1−N8	2.221(3)	Mn2−N7	2.236(3)
Mn1−N11	2.237(2)	Mn2−N14	2.227(2)
Mn1−N11A	2.205(3)	Mn2−N14B	2.221(3)
Mn1−N1	2.261(2)	Mn2−N3	2.267(2)
Mn1−N2	2.354(2)	Mn2−N4	2.361(2)
N5−N6	1.174(3)	N11−N12	1.197(3)
N6−N7	1.159(3)	N12−N13	1.144(3)
N8−N9	1.170(3)	N14−N15	1.191(3)
N9−N10	1.166(3)	N15−N16	1.152(3)
N5−Mn1−N11A	93.55(10)	N10−Mn2−N14B	92.59(11)
N5−Mn1−N8	88.65(11)	N10−Mn2−N14	94.63(10)
N11A−Mn1−N8	170.12(10)	N14B−Mn2−N14	78.89(10)
N5−Mn1−N11	96.16(10)	N10−Mn2−N7	88.42(11)
N11A−Mn1−N11	78.35(10)	N14B−Mn2−N7	175.67(11)
N8−Mn1−N11	91.84(10)	N14−Mn2−N7	96.83(11)
N5−Mn1−N1	170.79(10)	N10−Mn2−N3	169.36(11)
N11A−Mn1−N1	93.77(10)	N14B−Mn2−N3	97.49(10)
N8−Mn1−N1	85.08(10)	N14−Mn2−N3	90.65(9)
N11−Mn1−N1	90.80(9)	N7−Mn2−N3	81.78(10)
N5−Mn1−N2	101.63(10)	N10−Mn2−N4	103.93(10)
N11A−Mn1−N2	92.79(9)	N14B−Mn2−N4	90.81(9)
N8−Mn1−N2	96.20(10)	N14−Mn2−N4	159.20(9)
N11−Mn1−N2	160.61(9)	N7−Mn2−N4	93.04(10)
N1−Mn1−N2	72.43(9)	N3−Mn2−N4	72.65(9)
Mn1A−N11−Mn1	101.65(10)	Mn2B−N14−Mn2	101.11(10)
N6−N5−Mn1	124.0(2)	N6−N7−Mn2	140.4(3)
N9−N8−Mn1	141.8(2)	N9−N10−Mn2	125.5(2)
N12−N11−Mn1A	129.9(2)	N15−N14−Mn2B	130.0(2)
N12−N11−Mn1	127.4(2)	N15−N14−Mn2	128.9(2)
N7−N6−N5	177.2(3)	N13−N12−N11	179.8(4)
N10−N9−N8	176.7(3)	N16−N15−N14	179.1(3)

[a] Symmetry transformations: A, $-x, -y, -z$; B, $-x, -y+1, -z+1$.

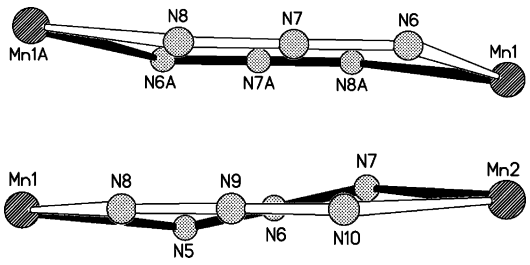

Figure 3. Views showing the different conformations of the double EE bridged $Mn(N3)_2Mn$ rings in **1** (top) and **2** (bottom).

In **2**, the two Mn(II) ions (Mn1, Mn2), one of the azido ligands (N8−N9−N10), and the center atom (N6) of the other form an approximate plane, and the other two azido nitrogens (N5 and N7) deviate from the plane by 0.244(4) and −0.192(4) Å, respectively. It is the first observation of nonparallel double EE azido bridges in Mn(II)−azido species. Several examples have been previously recognized in Ni(II) species.[15c,24] The Mn−azido−Mn torsion angles τ for the two azido ligands [37.2(2)° for N5−N6−N7 and 4.3(3)° for N8−N9−N10] are quite different from each other and from that in **1**. In the centrosymmetric double EO fragments, the bridging angles are 101.6(1)° for Mn1−N11−Mn1A and 101.1(1)° for Mn2−N14−Mn2B, somewhat larger than those in **1**. The Mn···Mn distances are 3.444 and 3.435 Å for the EO bridges and 5.465 Å for the EE ones. The shortest

(24) (a) Gao, E.-Q.; Liao, D.-Z.; Jiang Z.-H.; Yan S.-P.; Zhang, S.-F. *Acta Chim. Sin.* **2001**, *59*, 1294. (b) Chaudhuri, P.; Weyhermüller, T.; Bill, E.; Wieghardt, K. *Inorg. Chim. Acta* **1996**, *252*, 195. (c) Vicente, R.; Escuer, A.; Ribas, J.; Solans, X. *Inorg. Chem.* **1992**, *31*, 1726.

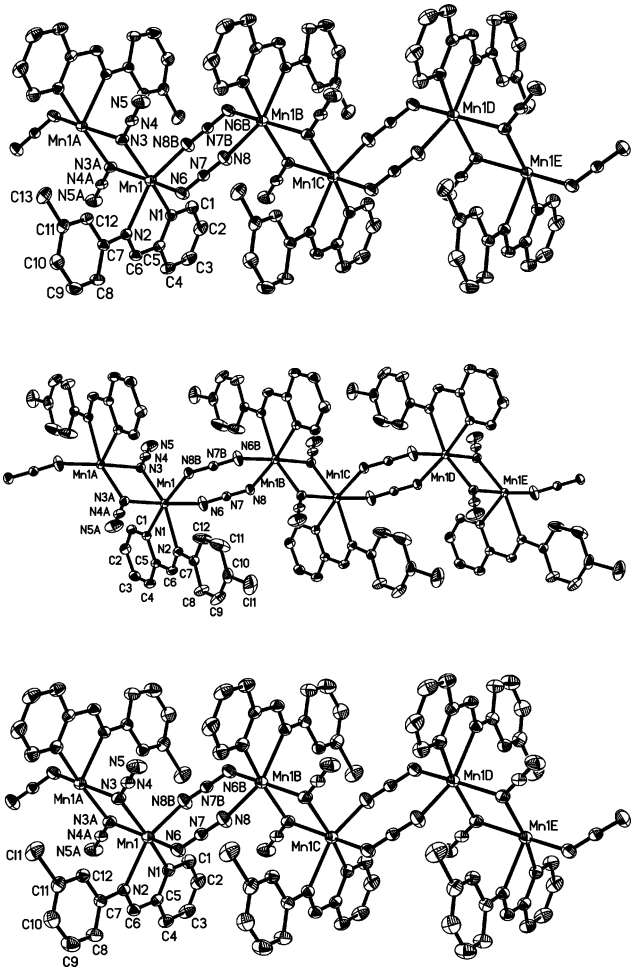

Figure 4. ORTEP views of the chain structures in **3** (top), **4** (middle), and **5** (bottom) with the atom labeling schemes.

interchain Mn···Mn distance is 8.653 Å between Mn1 and Mn2 ($x, y, z-1$).

Complexes **3**−**5** are isomorphous and also consist of parallel zigzag chains in which *cis*-octahedral Mn(II) ions are alternately linked by double EE and double EO bridges. The EO bridges are similar to those in **1** and **2**, and the EE bridging Mn−$(N_3)_2$−Mn fragments adopt the usual chair conformation with the two azido bridges parallel. The chain structures are depicted in Figure 4. Selected bond lengths and angles are given in Table 2 and some important bridging parameters in Table 4. As can been seen in Figures 1, 2 and 4, the orientation of the Schiff base ligands relative to the Mn(II)−azido chains seems to be dependent on the position of the substitution group in the phenyl ring. On one hand, for the unsubstituted (**1**) and *para*-substituted (**2** and **4**) ligands, the pyridyl groups are *trans* to an EE azido bridge and the imine group to an EO bridge. On the other hand, in the complexes (**3** and **5**) with *meta*-substituted ligands, the opposite situation is observed and the coordination geometry around metal ions exhibits a higher distortion from octahedral, as evidenced by the values of the N2−Mn1−N3 and N8B−Mn1−N2 angles. The Mn−N(EO)−Mn bridging angles in **3** and **5** are also significantly larger than those in the other complexes and represent the largest ones ever found in 1D Mn(II)−azido species containing double EO bridges.[16,17]

Table 4. Bridging and Magnetic Parameters for the Complexes

	EO			EE						
complex	M−N−M (deg)	M···M (Å)	J_F (cm^{-1})	M−N−N (deg)	M···M (Å)	τ (deg)	δ (deg)	M···N6[a] (Å)	J_{AF} (cm^{-1})	Θ (K)
1	99.6	3.406	3.8	130.7, 133.2	5.394	19.2	9.8	0.263	−15.4	−2.5
2	101.6	3.444	5.2	124.0, 140.4	5.465	37.2			−11.8	−1.4
	101.1	3.435		141.8, 125.5		4.3				
3	103.9	3.517	7.2	133.2, 126.5	5.310	36.2	19.5	0.509	−13.7	−1.1
4	100.6	3.413	4.1	133.1, 134.7	5.485	20.1	9.8	0.271	−13.3	−2.6
5	104.0	3.509	8.0	137.5, 125.7	5.332	23.2	12.0	0.316	−14.4	−1.5

[a] The distance from the metal ion to the plane defined by the two EE azido bridges.

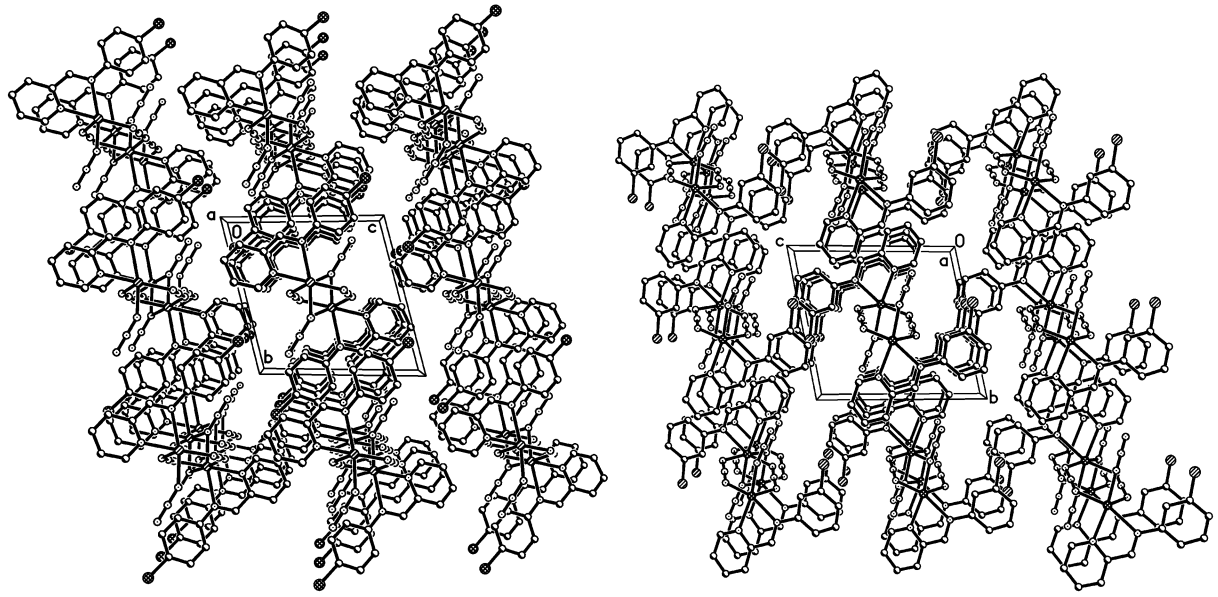

Figure 5. Views showing the packing of the chains in **4** (left) and **5** (right).

The substitution effects are also reflected in interchain distances. As illustrated by the packing diagram of **5** (Figure 5), the *meta*-substituted ligands in **3** and **5** are orientated so that the phenyl rings and the substitution groups lie between chains that pack along the *c* direction. As a consequence, the interchain Mn···Mn distances in this direction are 10.07 Å for **5** and 9.97 Å for **3**, much larger than the corresponding distances in **2** (8.81 Å) and **4** (8.59 Å). Compound **1** is excluded here because it is different from the others in crystal packing. The shortest interchain metal-to-metal distances in **3**−**5** are in the *b* direction, the values being 8.037, 8.209, and 8.012 Å, respectively.

Magnetic Properties. The magnetic susceptibilities of the five complexes were measured in the 2−300 K temperature range and are shown as χ_M and $\chi_M T$ versus T plots in Figure 6. The experimental $\chi_M T$ values at 300 K are between 3.56 and 3.82 emu mol^{-1} K, somewhat lower than the spin-only value (4.38 emu mol^{-1} K) expected for uncoupled high-spin Mn(II) ions. Upon cooling, the $\chi_M T$ products decrease monotonically and tend to zero at low temperature, while the χ_M values increase to rounded maximums at about 50 K and then decrease rapidly on further cooling. These features indicate a dominant antiferromagnetic interaction in these compounds. Despite the similarity in global magnetic behaviors, the maximum χ_M values of these five compounds vary significantly from 0.023 emu mol^{-1} around 56 K for **1** to 0.031 emu mol^{-1} around 46 K for **2**.

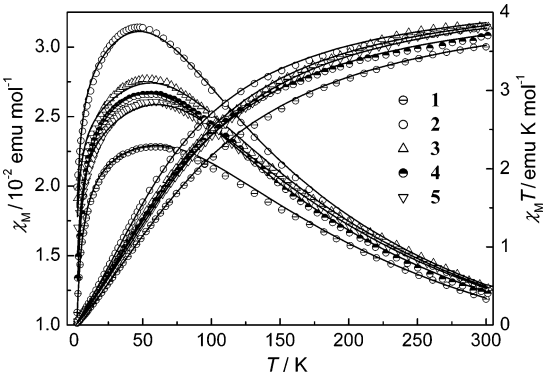

Figure 6. χ_M and $\chi_M T$ versus T plots for complexes **1**−**5**. The solid lines represent the best fit of the experimental data to eq 2.

According to the structural data, these compounds should exhibit alternating ferro- and antiferromagnetic interactions mediated by double EO and double EE azido bridges,[17] respectively. To simulate the experimental magnetic behavior, we used the theoretical model proposed by Cortés et al. for alternating F/AF $S = 5/2$ chains.[18b] The nearest neighbor exchange interactions are described by the spin Hamiltonian

$$\mathbf{H} = -J_1 \sum \mathbf{S}_{2i} \mathbf{S}_{2i+1} - J_2 \sum \mathbf{S}_{2i+1} \mathbf{S}_{2i+2} \qquad (1)$$

where J_1 and J_2 correspond to the alternating exchange constants for the EE and EO superexchange pathways, respectively, and the **S** operators are treated as classical

Table 5. Structural and Magnetic Parameters for Related 1D Mn(II)−Azido Complexes

complex[a]	Mn−N−Mn (deg)	J_F (cm^{-1})	δ (deg)	J_{AF} (cm^{-1})	ref
$[Mn(bipy)(N_3)_2]_n$[b]	101.0	9.6	22.7	−11.9	17b
$[Mn(bpm)(N_3)_2]_n$[b]	102.9	**4.1** (15.7)[f]	20.5	**−8.3** (−63.7)[f]	17d
$[Mn(dpa)(N_3)_2]_n$[b]	102.9	**5.2** (45.3)[f]	35.1	**−6.1** (−53.3)[f]	17e
$[Mn(3\text{-}bzpy)_2(N_3)_2]_n$[b]	100.4	3.5	26.6	−12.3	17a
$[Mn(3\text{-}Et,4\text{-}Mepy)_2(N_3)_2]_n$[b]	99.7	2.4	31.7	−13.7	17c
$[Mn(3\text{-}ampy)_2(N_3)_2(H_2O)]_n$[c]	99.6	2.3			16c
$[Mn_2(3\text{-}Et,4\text{-}Mepy)_6(N_3)_3]_n(PF_6)_n$[c]	101.4	3.3			16c
$[Mn(3\text{-}Etpy)_2(N_3)_2]_n$[d]			6.9	−11.7	16a
			11.6	−13.8	
$[Mn(pyOH)_2(N_3)_2]_n$[e]			38.0	−7.0	16a
$[Mn(3,5\text{-}lut)_2(N_3)_2]_n$[e]			32.2	−10.6	17a

[a] Abbreviations: bipy = 2,2′-bipyridine, bpm = bis(pyrazol-1-yl-)methane, dpa = 2,2′-dipyridylamine, 3-bzpy = 3-benzoylpyridine, 3-Et,4-Mepy = 3-ethyl-4-methylpyridine, 3-ampy = 3-aminopyridine, 3-Etpy = 3-ethylpyridine, pyOH = 2-hydroxypyridine, 3,5-lut = 3,5-dimethylpyridine. [b] Alternating double EE/double EO. [c] Alternating single EE/double EO. [d] Alternating double EE. [e] Uniform double EE. [f] The recalculated values are indicated in bold, and the values in parentheses are those reported in the references. See the text and Supporting Information for discussion.

spins. The deduced expression of the molar susceptibility is

$$\chi = [Ng^2\beta^2S(S+1)/(3kT)][(1+u_1+u_2+u_1u_2)/(1-u_1u_2)] \quad (2)$$

with $u_i = \coth[J_iS(S+1)/kT] - kT/[J_iS(S+1)]$ $(i = 1, 2)$.

The least-squares fits of the experimental data above 25 K to the above expression were acceptable, but when the low-temperature data were included in the fits, the agreement was not satisfactory, probably due to the presence of interchain antiferromagnetic interactions and/or zero-field splitting of the Mn(II) ion. Taking this into account, we introduced a Weiss constant Θ by replacing T with $T - \Theta$ in expression 2 (the T parameters in the u_i expression are not replaced). Following this approximation and fixing g to the expected value of 2.0 for Mn(II), satisfactory simulations were obtained in the whole temperature range. The best fit parameters are given in Table 4. The J_1 and J_2 parameters confirm alternating AF and F interactions with the AF one dominating, and the negative Θ values suggest small antiferromagnetic interchain interactions. For **2**, the structural data indicate two different ferromagnetic exchange constants corresponding to two different EO bridging fragments [Mn1−$(N_3)_2$−Mn1A and Mn2−$(N_3)_2$−Mn2B], but given the similar Mn−N−Mn bridging angles for the two fragments (101.1 vs 101.6°), an average ferromagnetic exchange constant was evaluated.

Magnetostructural Correlations. At this stage, it is desirable to deduce some information about magnetostructural correlations from the experimental data. Selected structural and magnetic data for previously reported Mn(II)−azido chains containing double EE and/or double EO bridges are collected in Table 5. It is noted that the J values reported for two of the compounds[17d,e] are anomalously large in comparison with the others. After checking the data carefully, we believe that the J values reported in ref 17e are actually for $JS(S+1)$ and that those in ref 17d seem to be in error.

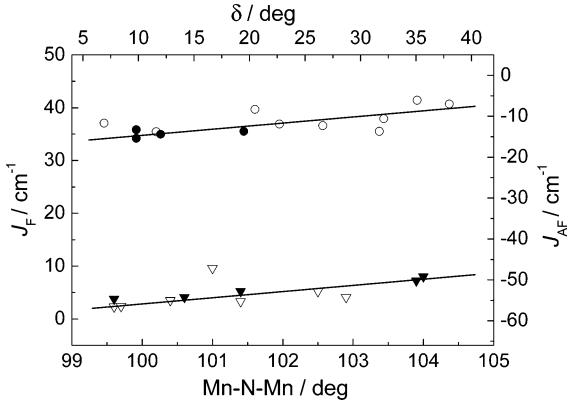

Figure 7. J_F against the bridging Mn−N−Mn angle (▽ and ▼) and J_{AF} against the dihedral δ angle (○ and ●). The solid symbols stand for the data in this work (Table 4) and the open ones for the data in Table 5. The solid lines are just guides for the eye.

We recalculated the J parameters by applying the $J_i \rightarrow J_iS(S+1)$ scaling factor[17b] for the former and by resimulating the original experimental data for the latter (see the Supporting Information for details). The new J values, indicated in bold in Table 5, are in good agreement with the experimental data and comparable with those for related Mn−azido compounds.

For the double EO bridging fragment, theoretical studies based on EHMO[17a,e] and DFT[25] calculations have indicated that the main factor controlling the magnitude of the ferromagnetic interaction should be the Mn−N−Mn bridging angle. The ferromagnetic interaction is expected to increase as the bridging angle increases. Using the data in Tables 4 and 5, the coupling constants were plotted against the bridging angles in Figure 7 (bottom). It seems that the experimental data follow this general trend. The dispersion of the data may be due to other factors such as Mn−N bond lengths, *cis* or *trans* coordination environments, and/or different properties of the coligands, which should influence the magnetic orbitals around the metal center. Besides, experimental uncertainties cannot be excluded. It is noteworthy that the present five complexes, which contain similar coligands and exhibit similar coordination enviroments, follow the general trend well (Figure 7, solid triangles).

As far as the EE bridging fragments are concerned, several variable parameters have been investigated for magnetostructural correlations:[17b,e,25] (i) M−N(azide) distances; (ii) M−N−N angles; (iii) the dihedral angle, δ, between the N(azido)−M−N(azido) plane and the mean plane defined by the two parallel azido bridges; (iv) the Mn−NNN−Mn torsion angle, τ. Complex **2** is unique in that the two EE azido ligands are not parallel. Magnetic analyses have suggested that an antiferromagnetic interaction is mediated via this type of double bridge, but more experimental examples are needed for magnetostructural correlation studies. For the double EE fragments in which the two azido bridges are parallel, the most useful parameter is the dihedral δ angle that defines the distortion of the Mn−(N−N−N)$_2$−

(25) Ruiz, E.; Cano, J.; Alvarez, S.; Alemany, P. *J. Am. Chem. Soc.* **1998**, *120*, 11122.

Mn ring from planarity toward the chair conformation. EHMO calculations[18a] have shown that the antiferromagnetic interaction between Mn(II) ions decreases with the distortion. DFT calculations for Ni(II) analogues have yielded the same prediction.[26] Figure 7 (top) shows the J_{AF} vs δ plot according to the experimental data in Table 5. All of the J_{AF} valves lie in a narrow range between -6.1 and -15.4 cm^{-1} with the δ angle varying from 6.9° to 38.0°. Although there is some dispersion, the general trend seems in agreement with the theoretical prediction; i.e., the larger the δ angle, the less negative the J_{AF} value. The dispersion may be due to the variations in other structural parameters, as well as experimental uncertainties. Among the present compounds, **1** and **4** exhibit identical δ (and similar τ) angles, but the antiferromagnetic coupling in **4** is somewhat weaker than that in **1**. The observation may be due to the larger average Mn−N−N angle (133.9° for **4** vs 132.2° for **1**) and/or the longer Mn−N(azido) distances (2.210 vs 2.198 Å) in **4**. The Mn···Mn distance in **4** is consequently significantly longer than that in **1** (5.485 vs 5.394 Å). The influence of the Mn−N distance on the magnetic interaction is self-evident, while EHMO calculations[25b] have demonstrated that the antiferromagnetic interaction should decrease for large Mn−N−N bond angles.

Conclusions

A series of azido-bridged Mn(II) complexes (**1**−**5**) have been prepared using five similar bidentate Schiff bases as auxiliary ligands and characterized crystallographically and magnetically. All five of the complexes consist of zigzag Mn(II)−azido chains in which the Mn(II) ions are alternately bridged by two EE and two EO azido ions. The double EO bridging moieties are similar with the bridging angles ranging from 99.6° to 104.0°. The Mn−(EE-N_3)$_2$−Mn ring in compound **2** adopts an unusual twist conformation with the two linear azido bridges crossing each other, while the rings in the other compounds take the usual chair conformation with the two azido bridges parallel. Magnetic analyses reveal that alternating ferro- and antiferromagnetic interactions are operative through the alternating EO and EE azido bridges. The J_F and J_{AF} parameters were evaluated to be in the 4.1−8.0 and -11.8 to -15.4 cm^{-1} ranges, respectively. The structural and magnetic data for these compounds and the related species in the literature are analyzed for the purpose of magnetostructural correlations. A general trend for the double EO bridge is followed; that is, the ferromagnetic interaction increases with the Mn−N−Mn bridging angle. The antiferromagnetic interaction through the double EE bridge is mainly dependent on the distortion of the Mn−(N_3)$_2$−Mn ring from planarity to the chair conformation: the larger the distortion, the weaker the antiferromagnetic interaction.

Acknowledgment. We are thankful for the financial support of NSFC (Grants 20201009 and 20001002) and MOST (Grant G19980613).

Supporting Information Available: An X-ray crystallographic file in CIF format and a PDF file concerning the revaluation of the *J* parameters for the compounds in refs 17d,e. This material is available free of charge via the Internet at http://pubs.acs.org.

IC0262987

(26) (a) de Biani, F. F.; Ruiz, E.; Cano, J.; Novoa, J. J.; Alvarez, S.*Inorg. Chem.* **2000**, *39*, 3221. (b) Escuer, A.; Vicente, R.; Goher M. A. S.; Mautner F. A. *Inorg. Chem.* **1996**, *35*, 6386.